
Journal of Information Display

ISSN: (Print) (Online) Journal homepage: https://www.tandfonline.com/loi/tjid20

# Flexible distributed Bragg reflectors as optical outcouplers for OLEDs based on a polymeric anode

Carmela Tania Prontera, Marco Pugliese, Roberto Giannuzzi, Sonia Carallo, Marco Esposito, Giuseppe Gigli & Vincenzo Maiorano

**To cite this article:** Carmela Tania Prontera, Marco Pugliese, Roberto Giannuzzi, Sonia Carallo, Marco Esposito, Giuseppe Gigli & Vincenzo Maiorano (2021) Flexible distributed Bragg reflectors as optical outcouplers for OLEDs based on a polymeric anode, Journal of Information Display, 22:1, 39-47, DOI: 10.1080/15980316.2020.1825537

**To link to this article:** https://doi.org/10.1080/15980316.2020.1825537



Published online: 08 Oct 2020.

JOURNAL OF INFORMATION DISPLAY
2021, VOL. 22, NO. 1, 39–47
https://doi.org/10.1080/15980316.2020.1825537



# Flexible distributed Bragg reflectors as optical outcouplers for OLEDs based on a polymeric anode

Carmela Tania Prontera[a], Marco Pugliese[a,b], Roberto Giannuzzi[a], Sonia Carallo[a], Marco Esposito[a], Giuseppe Gigli[a,b] and Vincenzo Maiorano[a]

[a]CNR NANOTEC - Institute of Nanotechnology, Lecce, Italy; [b]Dipartimento di Matematica e Fisica E. de Giorgi, Università Del Salento, Lecce, Italy

**ABSTRACT**
Top-emitting OLEDs (TOLEDs) represent a promising technology for the development of next-generation flexible and rollable displays, thanks to their improved light outcoupling and their compatibility with opaque substrates. Metal thin films are the most used electrodes for the manufacturing of TOLEDs, but they show poor resistance to mechanical deformation, which compromises the long-term durability of flexible devices. This paper reports the exploitation of a dielectric mirror (DBR) based on seven pairs of $TiO_2$ and $SiO_2$ combined with a polymeric electrode as an alternative to the bottom metal electrode in flexible TOLEDs. The DBR showed a maximum reflectivity of 99.9% at about 550 nm, and a stop-band width of about 200 nm. The reflectivity remained unchanged after bending and treatment with water and solvents. Green TOLED devices were fabricated on top of DBRs, and demonstrated good stability in terms of electro-optical and colorimetric characteristics, according to varying viewing angles. These results demonstrate that the combination of the flexible DBR with the polymeric anode is an interesting strategy for improving the durability of flexible TOLEDs for display applications, implemented on different kinds of free-standing ultra-thin substrates.

**ARTICLE HISTORY**
Received 6 July 2020
Accepted 8 September 2020

**KEYWORDS**
Top-emitting OLEDs; Distributed Bragg reflector; PEDOT-PSS anode; flexible optoelectronics

## 1. Introduction

In 1987, Tang and his co-workers demonstrated the first organic light emitting diode (OLED) that used an organic material as an emitter in a thin film electroluminescent device [1]. Since then, this kind of optoelectronic device has been extensively developed in both the academic and industrial fields for display and lighting applications. Indeed, OLEDs are dominating the display market, thanks to their multiple advantages: improved image quality (better contrast, higher brightness, wide viewing angle, wide color range, and fast refresh rate); low power consumption; and simple design that enables, in principle, the fabrication of thin, flexible, and even bendable displays [2,3]. Moreover, high-performance displays can be obtained by combining a pixelated matrix of OLEDs with a thin transistor layer that controls the switching of the individual pixels (active-matrix OLED or AMOLED) [4]. Usually, the opaque thin film transistor (TFT) array is manufactured on the substrate before the deposition of the materials of the OLED. For this reason, a top-emitting OLED (TOLED) is preferable for AMOLED structures [5,6]. Furthermore, in the top-emission architecture, the light is not trapped in the substrate with advantages in the light outcoupling [7–10]. The top-emitting structure also represents a solution for the integration of OLED devices in textiles, with interesting prospects for the development of wearable displays [11]. For all the mentioned reasons, TOLEDs are an ideal candidate for easy integration and engineering for the evolution of next-generation flexible displays.

The top-emitting configuration consists of a series of organic materials sandwiched between a thick, highly reflective bottom electrode and a semi-transparent top electrode that allows light emission [12]. Thin metal films are usually employed as electrodes for TOLEDs, thanks to their high conductivity and reflectivity that can be easily tuned by reducing their thickness, which is accompanied by an improvement in transparency. The transmittance of the semi-transparent top electrode can be further improved with the addition of a dielectric capping layer on top of it [13,14]. Unfortunately, thin metal films show poor resistance to mechanical deformation

**CONTACT** Marco Pugliese marco.pugliese@nanotec.cnr.it CNR NANOTEC – Institute of Nanotechnology, c/o Campus Ecotekne, via Monteroni, Lecce, 73100, Italy; Dipartimento di Matematica e Fisica E. de Giorgi, Università Del Salento, Campus Ecotekne, via Monteroni, Lecce, 73100, Italy

ISSN (print): 1598-0316; ISSN (online): 2158-1606

[15]. This lessens the durability of flexible OLEDs, due to which other kinds of electrode materials have to be preferred for flexible device manufacturing [16]. Thanks to its transparency in the visible range, tunable electrical conductivity, suitable work function, and high flexibility and stretchability, PEDOT:PSS is now the most used electrode material for flexible devices, besides being economically advantageous [17].

This paper demonstrates the possibility of realizing a TOLED based on a PEDOT:PSS bottom electrode deposited on top of a dielectric Bragg reflector (DBR)-modified flexible polyimide substrate. A DBR is a periodic structure obtained by alternating dielectric layers that can be used to obtain a high degree of reflection in a certain range of wavelengths, by exploiting the differences in the refractive indices of the dielectric layers and their thickness [18]. By combining the reflectivity properties of the DBR with the conductivity and flexibility of the polymeric electrode, flexible TOLEDs can be fabricated with the replacement of the bottom thin metal film electrode.

DBRs have been extensively used in combination with rigid OLED structures to study their microcavity effects on device performance [19–25]. Recently, a flexible TOLED was been fabricated on a metal foil substrate by using a DBR as an optical reflector and electrical insulating layer [26].

In this study, the DBR was deposited at room temperature through magnetron sputtering of seven pairs of $TiO_2$ and $SiO_2$ with appropriate thicknesses, in order to maximize the reflection in the emission wavelength region of the selected emitting material. The DBR showed excellent flexibility and resistance to water and organic solvents, as well as good surface properties. The PEDOT:PSS anode deposited on top of the flexible DBR showed good stability in terms of electrical resistance preservation after 1,000 bending cycles at a bending radius of 2.5 mm, which demonstrated its suitability as an electrode material for flexible devices, compared to traditional metal electrodes. To demonstrate the potential of the DBR as an outcoupler for flexible TOLEDs, green emitting devices were fabricated on top of it. To test the effect of a microcavity on the device characteristics, some preliminary investigations were carried out. The results showed that the luminance and efficiency values were strongly influenced by the total cavity thickness. Furthermore, the electroluminescence spectra of the devices at different viewing angles were evaluated. The best device for flexible display applications was identified, based on its good electro-optical performance, nearly Lambertian profile, and not significant color shift with the viewing angle. The reported results demonstrate the potential of a DBR structure as a strategic element of the development of flexible top-emitting devices.

## 2. Experimental section

### 2.1. Materials

The 50μm-thick flexible polyimide substrates were supplied by RS Components. The $SiO_2$ and $TiO_2$ sputtering targets were purchased from Kurt J. Lesker Company. Cesium was supplied by Saes Getters. Clevios PH1000 (PEDOT:PSS ratio = 1:2.5) was purchased from HeraeusCleviosGmbH, and was used as an anode. All the other materials used in the OLED device, i.e. N,N,N′,N′-Tetrakis(4-methoxyphenyl)benzidine (MeOTPD), 2,3,5,6 -Tetrafluoro-7,7,8,8-tetracyanoquinodimethane (F4TC NQ), 2,2′,2ʺ(1,3,5-Benzinetriyl)-tris(1-phenyl-1-H-ben zimidazole) (TPBi), Tris[2-phenylpyridinato-C2,N]iridi um(III) ($Ir(ppy)_3$), Bathophenanthroline (BPhen), silver (Ag), and tungsten (VI) oxide ($WO_3$) were purchased by Sigma Aldrich.

### 2.2. DBR and OLED fabrication

The flexible substrates were cleaned with acetone, isopropyl alcohol, and deionized water and dried with Nitrogen gas. To further eliminate impurities on top of the flexible substrates and to improve the adhesion, 2’ oxygen plasma treatments (50 W, 30 sscm) were performed on top of the substrates before starting the DBR growth. To fabricate the DBR, seven pairs of $TiO_2/SiO_2$ (54 nm/91 nm) were deposited on the flexible substrates via sputtering deposition at 250 W (room temperature, 30 sccm of argon). The OLED structure on top of the DBR had the following components: PEDOT:PSS/p doped MeOTPD (F4TCNQ)/MeOTPD/TPBi:$Ir(ppy)_3$/BPhen/n doped BPhen (Cs)/Ag/$WO_3$. The anode layer consisted of a thin film of PEDOT:PSS (100 nm) that was obtained via spin coating deposition (1,000 rpm x 60”) of a commercial solution, which was modified with the addition of 5% by volume of dimethyl sulfoxide (DMSO) to improve the conductivity, and with a successive annealing process at 120°C for 1 h. The other organic layers, Ag and $WO_3$, were deposited via thermal evaporation in a Kurt J. Lesker multiple high-vacuum chamber system.

### 2.3. Characterization

The optical constants and thickness of the used materials were measured using a J.A. Wollam M-2000XI ellipsometer.

The reflectance spectra of the DBR were measured using a Perkin Elmer UV/Vis/NIR spectrometer (Lambda 1050) equipped with a 150 mm InGaAs Integration Sphere. To test the flexibility and stability of the DBR, the reflectance spectra were measured after the following stress conditions: 100 bending cycles with a curvature radius of 2.5 mm and water/solvent dropping. Water, isopropyl alcohol, chloroform, and toluene were used to test the solvent stability of the DBR structure. In particular, 1 ml of liquid was dropped on top of the DBR surface; and after about 1 min, the sample was dried with a nitrogen flow, and the reflectance spectrum was measured.

The DBR cross-section was caught via scanning electron microscopy (Zeiss FE-SEM Merlin). The surface characteristics of the DBR were evaluated via scanning electron microscopy (Zeiss FE-SEM Merlin) and atomic force microscopy (no-contact mode, AFM PARK SYSTEMS XE-100).

Electrical resistance measurements were carried out on 7 cm x 0.5 cm anode strips (Polyimide /DBR/100 nm PEDOT:PSS and polyimide /100 nm thermal evaporated Ag) using a 2420 Keithley source meter.

The optoelectronic characteristics of the OLED devices were measured in a glove box using an Optronics OL770 spectrometer coupled to the OL610 telescope unit with an optical fiber for the luminance measurements. The whole system was calibrated by the National Institute of Standards and Technology (NIST) using a standard lamp, and was directly connected by an RS232 cable to a Keithley 2420 current–voltage source meter. The electroluminescence spectra at different angles were measured by coupling the sample holder with a goniometer, and then rotating the sample to acquire its emission from 0 to 60 degrees, first clockwise and then counter-clockwise.

## 3. Result and discussion

A DBR is a multilayer structure of two alternating dielectric materials with different refractive indices. The reflectivity of a DBR is very high in a specific range of wavelengths (stop-band), and reaches its maximum at the wavelength equal to four times the optical thickness of each layer. In these conditions, the reflections at the interface of the different layers combine with constructive interference, and the structure acts as a high-quality reflector. The reflectivity of the mirror is determined in particular by the contrast of the refractive index between the materials and by the number of alternating pairs. Considering these aspects, to fabricate a highly reflective DBR, $TiO_2$ and $SiO_2$ were chosen as high refractive index and low refractive index materials, respectively. The $TiO_2$ and $SiO_2$ layers were deposited via room temperature magnetron sputtering deposition, and their optical constants were measured as a function of their wavelength via spectroscopic ellipsometry (Figure 1a). The thickness values of $TiO_2$ and $SiO_2$ in the DBR were calculated using the following formula: $d\ \lambda/4n$, wherein $d$ is the layer thickness, $\lambda$ is the optimized DBR reflectance wavelength, and $n$ is the refractive index at the specific selected wavelength. The DBR on top of the flexible substrate consisted of seven pairs of $TiO_2$ and $SiO_2$, and their thickness values were designed to maximize the reflection in the emission region of the material chosen as the emitter [$Ir(ppy)_3$, peak emission @525 nm].

In Figure 1b, the reflectance spectrum of the DBR is reported. It shows a maximum reflectance of 99.9% at about 540 nm, and a stop-band width of about 200 nm, which demonstrate the suitability of such DBR to act as a bottom reflector for TOLED architectures. The reflectance spectrum remained unchanged even after 100 bending cycles (2.5 mm curvature radius) and after treatment with water and various organic solvents, which demonstrated the extreme flexibility of the DBR structure and its compatibility with solvent-based deposition techniques (Figure 1b). In particular, this last aspect opens perspectives towards the development of top-emitting devices by using high-throughput printing deposition techniques with a significant reduction in production costs.

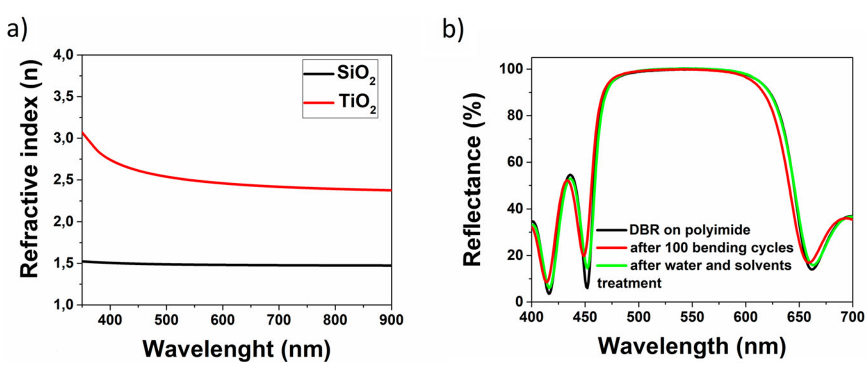


**Figure 1.** Optical characteristics of the sputtered layers and the DBR multilayer: a) refractive index of the $TiO_2$ and $SiO_2$ thin films; and b) reflectance spectra of the pristine seven pairs of $TiO_2/SiO_2$ DBR and the after-stress conditions (100 bending cycles at a 2.5 mm curvature radius and water/organic solvents dropping).

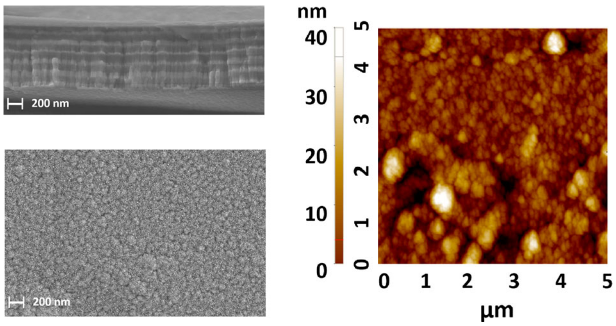


**Figure 2.** Morphological characterization of the seven pairs of $TiO_2/SiO_2$ DBR structure: a) SEM cross-section; b) SEM image of the DBR surface; and c) AFM picture of the DBR surface.

The cross-section of the DBR (Figure 2a) evaluated via scanning electron microscopy (SEM) further demonstrates the good reproducibility of the deposition processes, which points out the excellent optical properties of the final mirror, as already evaluated from the reflection spectrum. The SEM image of the DBR surface (Figure 2b) denotes a granular morphology with a grain size in the order of tens of nanometers. The AFM characterization confirms the granular structure, and a roughness of 9 nm was observed for the DBR surface, which is suitable for the growth of the OLED structure (Figure 2c).

OLEDs were fabricated on top of the flexible DBRs to demonstrate their potential as a reflective structure for TOLEDs (Figure 3).

PEDOT:PSS was selected as the anode layer for the TOLED device, due to its good conductivity and outstanding flexibility on account of its polymeric nature. Furthermore, the anode based on PEDOT:PSS was obtained starting from a solution-based deposition. For this reason, it is an ideal candidate as an electrode for the realization of printed flexible devices. To demonstrate the suitability of the polymeric anode for the fabrication of flexible devices, its electrical resistance variation was evaluated in bending conditions, and a 100 nm thin silver film was used as reference. The PEDOT:PSS thin film deposited on top of the flexible DBR showed an increment of its electrical resistance of about 15%

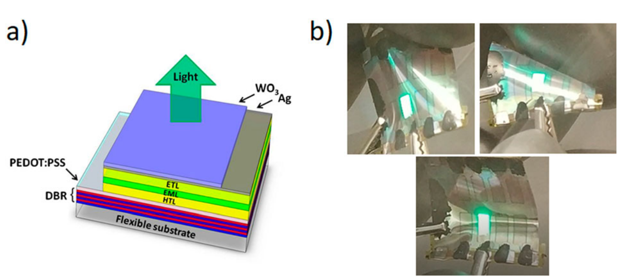


**Figure 3.** Device on the DBR structure: a) device architecture; and b) pictures of Dev3 powered at 4 V.

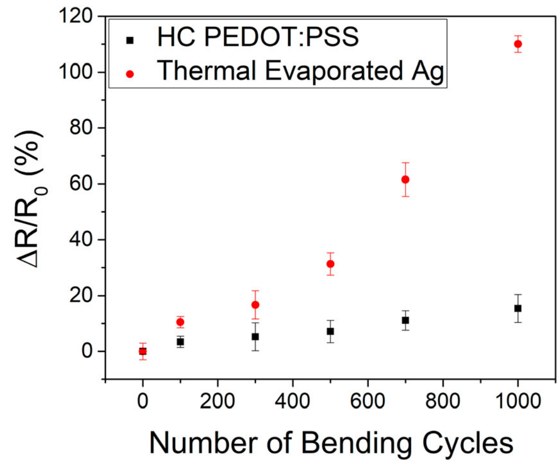


**Figure 4.** Percentage resistance variation as a function of the number of bending cycles measured on the polyimide/DBR/PEDOT:PSS and polyimide /thermal evaporated silver strips (width, 0.5 cm and length, 7 cm).

after 1,000 bending cycles, with a curvature radius of 2.5 mm; whereas in the same stress conditions, the thin silver film showed an improvement of more than 100% (Figure 4). Such results confirm the superior flexibility of PEDOT:PSS with respect to metallic electrodes, as already reported in literature [15,27,28].

The structure of the TOLED devices consisted of the following layers: HC (highlyconductive) PEDOT:PSS/p-doped MeOTPD/MeOTPD/TPBi:Ir(ppy)$_3$/BPhen/n-doped BPhen/Ag/$WO_3$. The top thin silver layer combined with the $WO_3$ capping layer acted as a semitransparent top electrode; and to optimize the transmittance, their thickness values were calculated through numerical simulation using ETFOS software (by Fluxim) [29]. Different thickness values of p-doped MeOTPD and n-doped BPhen were deposited to evaluate the effect of the cavity thickness on the device performance. In Table 1, the structures of the fabricated OLEDs (Dev1, Dev2, and Dev3) are reported.

The Current Density vs. Voltage, Luminance vs. Voltage, and Efficiency vs. Voltage curves of all the devices are reported in Figures 5a-b-c. The maximum current density value of all the devices was around 70 mA/cm$^2$, whereas the luminance values ranged from 200 to 3,000 cd/m$^2$, and the efficiency, between 0.3 and 4 cd/A. Such large differences in the luminance and efficiency values are attributable to the different resonance conditions within the cavity devices. Indeed, the top-emitting devices were composed of the combined DBR and PEDOT:PSS contact, organic layers, and a semi-transparent top contact. The latter showed strong reflection due to the large refractive index mismatches with the organic layer. As a result, these OLEDs consisted

**Table 1.** Structures of the fabricated OLED devices.

| Device | PEDOT:PSS (nm) | *p*-doped HTL (nm) | HTL (nm) | EML (nm) | ETL (nm) | n-doped ETL (nm) | Cathode Ag/$WO_3$ (nm/nm) | Total device length (nm) |
|---|---|---|---|---|---|---|---|---|
| Dev1 | 100 | 20 | 10 | 25 | 10 | 20 | 12/35 | 185 |
| Dev2 | 100 | 40 | 10 | 25 | 10 | 40 | 12/35 | 225 |
| Dev3 | 100 | 50 | 10 | 25 | 10 | 50 | 12/35 | 245 |

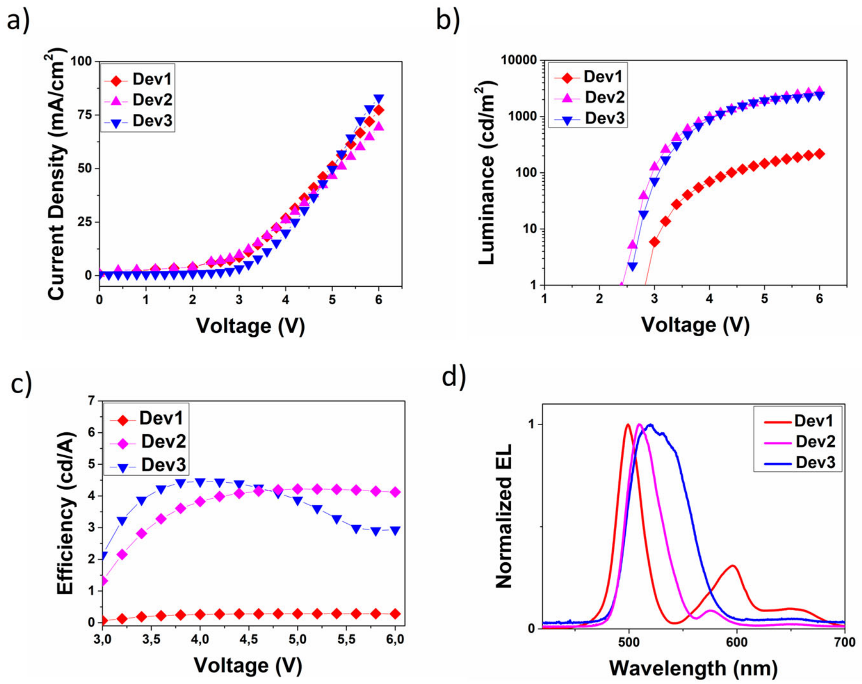


**Figure 5.** Electro-optical characterization of the fabricated OLEDs: a) Current Density vs. Voltage curves; b) Luminance vs. Voltage curves; c) Efficiency vs. Voltage curves; and d) Normalized electroluminescence (EL) spectra at 0°.

of a structure formed by two reflecting faces on two sides of an optical medium (organic materials) that formed a microcavity, which strongly influenced the device performance [30–32].

In a cavity OLED device, the higher luminance values are usually observed when the cavity length is equal to $\lambda/2n$ and its multiples, wherein $\lambda$ is the emission wavelength of the emitting material, and $n$ is the refractive index of the organic stack of the device. For higher and lower thickness values, the luminance values are lower because the optimal resonance conditions are not respected [33–35].

Higher luminance and efficiency values were observed for Dev2 and Dev3 with cavity lengths of 225 and 245 nm, respectively, close to $\lambda/n$ resonance conditions [36]. Dev1 did not match the best resonance conditions, so there was a drop in the luminance and efficiency values. In Figure 5d, the electroluminescence spectra of all the devices are reported. Dev1 and Dev2 have a narrow peak at 500 and 509 nm, respectively, and a secondary peak shifted in the red region with respect to the principal one. Dev3 shows a larger emission peak, with the maximum at 520 nm.

Moreover, a microcavity usually has a significant impact on the emissive properties of an OLED device at different viewing angles. In a Fabry–Perot resonator, the cavity mode wavelength decreases with an increasing viewing angle according to: $\lambda = 2\pi\ m\ L\ n\ cos(\theta)$, wherein $\lambda$ is the resonance wavelength, $m$ is the mode number, $n$ is the refractive index, $L$ is the cavity length, and $\theta$ is the internal angle that is related to the viewing angle of the microcavity through Snell's law [37,38]. The blue shift effect is more consistent with the improvement of the cavity thickness and when DBR mirrors are used [20,39,40]. As for the spatial distribution of the emission intensity, the higher the reflectance of the mirrors is, the more concentrated the emission intensity will be on the cavity axis, with a large deviation from the classical Lambertian behavior observed for traditional OLEDs (sub-Lambertian) [41,42]. Furthermore, when moving from ideal resonance conditions, the maximum emission is observed at angles greater than 0° – a behavior called *super-Lambertian* [42]. Figure 6 shows the electroluminescent spectra at different viewing angles; and Figure 7, the CIE coordinates and the electroluminescent intensity at different viewing angles. In Dev1,

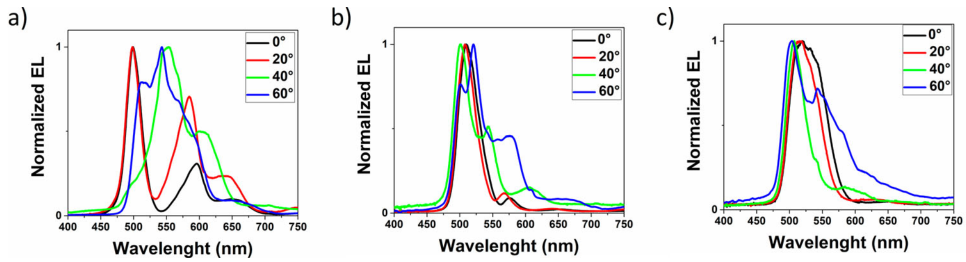


**Figure 6.** Normalized electroluminescence spectra from 0° to 60° for a) Dev1, b) Dev2, and c) Dev3.

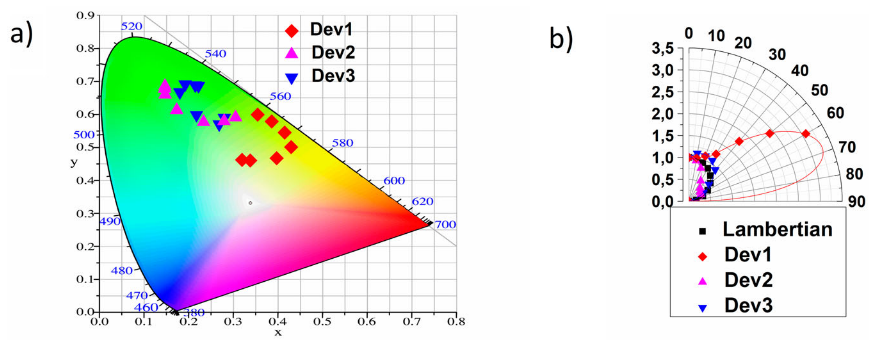


**Figure 7.** a) CIE coordinates diagram at different viewing angles (from 0° to 60°); and b) Emission profile in polar coordinates.

with the increase in the viewing angle, the secondary peak observed at 0° shows an increase in intensity and a shift in the blue region of the spectrum, whereas the peak at 500 nm tends to disappear. The electroluminescence spectra of Dev2 show a trend similar to that observed in Dev1, with further peaks that appear at high viewing angles. The electroluminescence spectrum of Dev3 at 0° and 20° is larger than that of Dev2 and Dev3 at the same angles, and it starts to narrow at 40°, with a consistent secondary peak observed at about 540 nm at 60°.

The aforementioned behaviors, related to the well-known photon-like angular dispersion of the cavity mode, obviously induce a variation of the CIE coordinates with the viewing angles. As reported in Figure 7a, Dev1 and Dev2 show larger color variations, whereas Dev3 shows a less consistent color shift. However, in all the devices, the color shift is not very significant, and the emission remains in the green region of the spectrum.

The angular emission profile was also evaluated. Dev1 and Dev3 have a super-Lambertian profile, with a maximum emission intensity at 60° and 10°, respectively. Dev2 shows a sub-Lambertian profile, with a maximum emission at 0°.

All these data demonstrate that the right compromise between optical efficiency, color purity, and an angular color shift must be found, and the best microcavity device suitable for display applications must be identified.

Dev3 shows the highest efficiency value, a nearly Lambertian emission profile, and a limited color shift with the viewing angle. For these reasons, Dev3 represents the best solution for flexible display applications, based on a flexible DBR combined with a PEDOT:PSS anode. Further investigations must be carried out to improve the device performance by properly evaluating the thickness of each layer.

## 4. Conclusions

Flexible TOLEDs based on a PEDOT:PSS anode layer combined with a highly reflective DBR were fabricated on 50µm-thin polyimide substrates. Indeed, the polymeric anode is the best solution for the manufacturing of flexible devices as a substitute for the commonly used thin metal films that show poor resistance to mechanical deformation. If opportunely designed, DBRs show higher reflectivity with respect to thin metal films, and the stopband can be easily tuned according to the selected emitting materials. For such reasons, DBRs are an extremely versatile solution for TOLEDs. In this study, the DBR structure was designed and optimized to maximize the reflection properties in the green wavelength region. The reflectivity of the DBR did not change after bending and the water/solvent treatments, demonstrating the high flexibility of DBR and its compatibility with solution-based deposition processes. The TOLEDs that were obtained by combining the reflective properties of the DBR with the conductivity of the PEDOT:PSS showed an electro-optical performance that can be opportunely tuned by considering the microcavity effects. In particular, the best OLED showed an not significant color shift with different viewing angles and a nearly-Lambertian emission profile. For these reasons, the best OLED is a good candidate for flexible and rollable display applications. As a future prospect, since DBRs are composed of oxide materials that are typically used for thin film encapsulation of flexible organic devices, the deposition processes can be optimized to obtain barrier layers and combine the encapsulating and outcoupling properties in a single multilayer structure.

In conclusion, DBRs are interesting functional elements that can be appropriately combined with flexible optoelectronic devices based on polymeric electrodes to improve their performance, versatility, and durability.

## Acknowledgments

This work was supported by the FISR-CNR national project 'Tecnopolo di nanotecnologia e fotonica per la medicina di precisione' - CUP B83B17000010001 and the Apulia regional project 'MOSAICOS - MOSAici Interattivi eCO-Sostenibili', Cod. HOQ3PM3 - CUP B37H17004900007

## Disclosure statement

No potential conflict of interest was reported by the authors.

## Notes on contributors

***Carmela Tania Prontera*** received her BSc and MSc degrees in Chemistry from the University of Bari, Italy in 2009 and 2012, respectively; and her PhD degree in Chemical Science from the University of Naples, Italy in 2019. Since December 2018, she has been working at CNR Nanotec in Lecce. Her research activity is focused on the development of integrated optoelectronic devices (organic light emitting diodes or OLEDs, electrochromic devices, etc.) for the development of innovative technologies in the fields of 'smart windows' and 'wearable electronics'.

***Marco Pugliese*** holds an MSc degree in Telecommunication Engineering and is currently a PhD student in Physics and Nanotechnology at the University of Salento, Italy. He works on the development of advanced multifunctional optoelectronic devices (OLEDs and electrochromic devices) for smart windows applications.

***Roberto Giannuzzi*** received his MSc degree in Materials Engineering from the University of Salento, Lecce in 2009; and his PhD degree in Bio-Molecular Nanotechnology from the Italian Institute of Technology in Lecce in 2013. He is currently a research fellow at CNR Nanotec. His research interests include electrochemical fabrication of nanostructured materials and thin films, electrochemistry, and (spectro)electrochemistry of semiconductors.

***Sonia Carallo*** is a staff technician at CNR Nanotec. She has extensive experience in the morphological characterization of thin films and in the fabrication of optoelectronic devices.

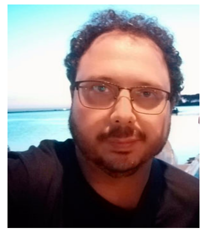

***Marco Esposito*** is a staff researcher at CNR Nanotec. He graduated with a BSc degree in Telecommunication Engineering and a PhD degree in Materials, Structures, and Nanotechnologies Engineering. He has developed skills in advanced photonic and plasmonic nanostructure engineering by exploiting two- and three-dimensional nanofabrication techniques, such as electron beam lithography, focused on ion/electron beam-induced deposition, together with optical and morphological characterization, and the FDTD-based simulation method. His research interest is focused on the development of novel nanostructure architectures for photonic applications.

***Giuseppe Gigli*** took the MSc degree in Physics at the University of Rome (IT) 'La Sapienza' in 1996 and the Ph.D. in Physics in 1999 at the University of Lecce (IT). Since 2001 he is Lecturer in Physics in the Engineering Faculty of the University of Salento, where he is full Professor since 2010. He is the Director of the CNR Institute of Nanotechnology, where he is also coordinator of the Molecular Nanotechnology group. His main research activities involve: study and fabrication of organic optoelectronic/photonic devices, microfluidic laboratories on chip (LOCs) and drug delivery systems for advanced theranostics.

***Vincenzo Maiorano*** received his MSc degree in Physics from the University of Lecce in 2003. Since 2007, he has been a research technologist at CNR Nanotec. His main research activities are studies of supramolecular aggregates in organic semiconductors; design, fabrication, and characterization of electroluminescent devices (OLED OLEFET); and design, fabrication, and characterization of semi-transparent smart panels showing color modulation, in which energy production (solar cells), lighting (OLEDs), and solar control/sun screening (photovoltacromics) are combined.

## References

[1] C.W. Tang, and S.A. Vanslyke, Organic Electroluminescent Diodes, Appl. Phys. Lett. **51** (12), 913–915 (1987). doi:10.1063/1.98799.
[2] S.-J. Zou, Y. Shen, F.-M. Xie, J.-D. Chen, Y.-Q. Li, and J.-X. Tang, Recent Advances in Organic Light-Emitting Diodes: Toward Smart Lighting and Displays, Mater. Chem. Front **4** (3), 788–820 (2020). doi:10.1039/C9QM00716D.
[3] Y.F. Liu, J. Feng, Y.G. Bi, D. Yin, and H.B. Sun, Recent Developments in Flexible Organic Light-Emitting

Devices, Adv. Mater. Technol. **4** (1), 1–19 (2019). doi:10.1002/admt.201800371.
[4] W.F. Aerts, S. Verlaak, and P. Heremans, Design of an Organic Pixel Addressing Circuit for an Active-Matrix OLED Display, IEEE Trans. Electron Devices **49** (12), 2124–2130 (2002). doi:10.1109/TED.2002.805565.
[5] J.S. Yoo, S.H. Jung, Y.C. Kim, S.C. Byun, J.M. Kim, N.B. Choi, S.Y. Yoon, C.D. Kim, Y.K. Hwang, and I.J. Chung, Highly Flexible AM-OLED Display with Integrated Gate Driver Using Amorphous Silicon TFT on Ultrathin Metal Foil, IEEE/OSA J. Disp. Technol. **6** (11), 565–570 (2010). doi:10.1109/JDT.2010.2048998.
[6] S.K. Hong, J.H. Sim, I.G. Seo, K.C. Kim, S.I. Bae, H.Y. Lee, N.Y. Lee, and J. Jang, New Pixel Design on Emitting Area for High Resolution Active-Matrix Organic Light-Emitting Diode Displays, IEEE/OSA J. Disp. Technol. **6** (12), 601–606 (2010). doi:10.1109/JDT.2010.2063694.
[7] J.N. Bardsley, International OLED Technology Roadmap, IEEE J. Sel. Top. Quantum Electron. **10** (1), 3–9 (2004). doi:10.1109/JSTQE.2004.824077.
[8] W. Brütting, J. Frischeisen, T.D. Schmidt, B.J. Scholz, and C. Mayr, Device Efficiency of Organic Light-Emitting Diodes: Progress by Improved Light Outcoupling, Phys. Status Solidi Appl. Mater. Sci. **210** (1), 44–65 (2013). doi:10.1002/pssa.201228320.
[9] L.H. Smith, J.A.E. Wasey, and W.L. Barnes, Light Outcoupling Efficiency of Top-Emitting Organic Light-Emitting Diodes, Appl. Phys. Lett. **84** (16), 2986–2988 (2004). doi:10.1063/1.1712036.
[10] C.J. Yang, C.L. Lin, C.C. Wu, Y.H. Yeh, C.C. Cheng, Y.H. Kuo, and T.H. Chen, High-Contrast Top-Emitting Organic Light-Emitting Devices for Active-Matrix Displays, Appl. Phys. Lett. **87** (14), 1–3 (2005). doi:10.1063/1.2081137.
[11] S. Choi, S. Kwon, H. Kim, W. Kim, J.H. Kwon, M.S. Lim, H.S. Lee, and K.C. Choi, Highly Flexible and Efficient Fabric-Based Organic Light-Emitting Devices for Clothing-Shaped Wearable Displays, Sci. Rep. **7** (1), 1–8 (2017). doi:10.1038/s41598-017-06733-8.
[12] S. Hofmann, M. Thomschke, B. Lüssem, and K. Leo, Top-Emitting Organic Light-Emitting Diodes, Opt. Express **19** Suppl 6 (November), A1250–64 (2011). doi:10.1364/OE.19.0A1250.
[13] S.D. Yambem, M. Ullah, K. Tandy, P.L. Burn, and E.B. Namdas, ITO-Free Top Emitting Organic Light Emitting Diodes with Enhanced Light out-Coupling, Laser Photonics Rev. **8** (1), 165–171 (2014). doi:10.1002/lpor.201300148.
[14] Q. Huang, K. Walzer, M. Pfeiffer, K. Leo, M. Hofmann, and T. Stübinger, Performance Improvement of Top-Emitting Organic Light-Emitting Diodes by an Organic Capping Layer: An Experimental Study, J. Appl. Phys. **100** (6), (2006). doi:10.1063/1.2338145.
[15] X. Luo, B. Zhang, and G. Zhang, Fatigue of Metals at Nanoscale: Metal Thin Films and Conductive Interconnects for Flexible Device Application, Nano Mater. Sci. **1** (3), 198–207 (2019). doi:10.1016/j.nanoms.2019.02.003.
[16] S. Sharma, S. Shriwastava, S. Kumar, K. Bhatt, and C.C. Tripathi, Alternative Transparent Conducting Electrode Materials for Flexible Optoelectronic Devices, Optoelectronics Rev. **26** (3), 223–235 (2018). doi:10.1016/j.opelre.2018.06.004.
[17] X. Fan, W. Nie, H. Tsai, N. Wang, H. Huang, Y. Cheng, R. Wen, L. Ma, F. Yan, and Y. Xia, PEDOT:PSS for Flexible and Stretchable Electronics: Modifications, Strategies, and Applications, Adv. Sci. **6** (19), (2019). doi:10.1002/advs.201900813.
[18] D.-X. Wang, I.T. Ferguson, J.A. Buck, and D. Nicol, Optical Design and Simulation for Nanoscale Distributed Bragg Reflector (DBR) for High-Brightness LED, Nanoeng. Fabr. Prop. Opt. Devices III **6327** (2), 63270Q (2006). doi:10.1117/12.674678.
[19] Y. Hu, J. Lin, L. Song, Q. Lu, W. Zhu, and X. Liu, Vertical Microcavity Organic Light-Emitting Field-Effect Transistors, Sci. Rep. **6** (March), 1–8 (2016). doi:10.1038/srep23210.
[20] K. Neyts, P. De Visschere, D.K. Fork, and G.B. Anderson, Semitransparent Metal or Distributed Bragg Reflector for Wide-Viewing-Angle Organic Light-Emitting-Diode Microcavities, J. Opt. Soc. Am. B. **17** (1), 114 (2000). doi:10.1364/josab.17.000114.
[21] F.S. Juang, L.H. Laih, C.J. Lin, and Y.J. Hsu, Angular Dependence of the Sharply Directed Emission in Organic Light Emitting Diodes with a Microcavity Structure, Japanese J. Appl. Physics, Part 1 Regul. Pap. Short Notes Rev. Pap. **41** (4 B), 2787–2789 (2002). doi:10.1143/JJAP.41.2787.
[22] J. Zhang, H. Zhang, Y. Zheng, M. Wei, H. Ding, B. Wei, and Z. Zhang, Super Color Purity Green Organic Light-Emitting Diodes with ZrO2/Zircone Nanolaminates as a Distributed Bragg Reflector Deposited by Atomic Layer Deposition, Nanotechnology **28** (4), (2017). doi:10.1088/1361-6528/28/4/044002.
[23] Y. Wu, J. Yang, S. Wang, Z. Ling, H. Zhang, and B. Wei, High-Performance White Organic Light-Emitting Diodes Using Distributed Bragg Reflector by Atomic Layer Deposition, Appl. Sci. **9** (7), (2019). doi:10.3390/app9071415.
[24] A. Genco, G. Giordano, S. Carallo, G. Accorsi, Y. Duan, S. Gambino, and M. Mazzeo, High Quality Factor Microcavity OLED Employing Metal-Free Electrically Active Bragg Mirrors, Org. Electron **62** (March), 174–180 (2018). doi:10.1016/j.orgel.2018.07.034.
[25] T. Kitabayashi, T. Asashita, N. Satoh, T. Kiba, M. Kawamura, Y. Abe, and K.H. Kim, Fabrication and Characterization of Microcavity Organic Light-Emitting Diode with CaF2/ZnS Distributed Bragg Reflector, Thin Solid Films **699** (March), 137912 (2020). doi:10.1016/j.tsf.2020.137912.
[26] K. Hong, H.K. Yu, I. Lee, S. Kim, Y. Kim, K. Kim, and J.L. Lee, Flexible Top-Emitting Organic Light Emitting Diodes with a Functional Dielectric Reflector on a Metal Foil Substrate, RSC Adv. **8** (46), 26156–26160 (2018). doi:10.1039/c8ra05759a.
[27] H.Y. Lee, S.M. Yi, J.H. Lee, H.S. Lee, S. Hyun, and Y.C. Joo, Effects of Bending Fatigue on the Electrical Resistance in Metallic Films on Flexible Substrates, Met. Mater. Int. **16** (6), 947–951 (2010). doi:10.1007/s12540-010-1213-2.
[28] M. Borghetti, M. Ghittorelli, E. Sardini, M. Serpelloni, and F. Torricelli, Electrical Characterization of PEDOT: PSS Strips Deposited by Inkjet Printing on Plastic Foil

for Sensor Manufacturing, IEEE Trans. Instrum. Meas. **65** (9), 2137–2144 (2016). doi:10.1109/TIM.2016.2571518.

[29] P. Cossari, M. Pugliese, S. Gambino, A. Cannavale, V. Maiorano, G. Gigli, and M. Mazzeo, Fully Integrated Electrochromic-OLED Devices for Highly Transparent Smart Glasses, J. Mater. Chem. C. **6** (27), 7274–7284 (2018). doi:10.1039/c8tc01665 h.

[30] H. Riel, S. Karg, T. Beierlein, B. Ruhstaller, and W. Rieß, Phosphorescent Top-Emitting Organic Light-Emitting Devices with Improved Light Outcoupling, Appl. Phys. Lett. **82** (3), 466–468 (2003). doi:10.1063/1.1537052.

[31] H. Riel, S. Karg, T. Beierlein, W. Rieß, and K. Neyts, Tuning the Emission Characteristics of Top-Emitting Organic Light-Emitting Devices by Means of a Dielectric Capping Layer: An Experimental and Theoretical Study, J. Appl. Phys. **94** (8), 5290–5296 (2003). doi:10.1063/1.1605256.

[32] C.W. Chen, P.Y. Hsieh, H.H. Chiang, C.L. Lin, H.M. Wu, and C.C. Wu, Top-Emitting Organic Light-Emitting Devices Using Surface-Modified Ag Anode, Appl. Phys. Lett. **83** (25), 5127–5129 (2003). doi:10.1063/1.1635076.

[33] C.L. Lin, H.C. Chang, K.C. Tien, and C.C. Wu, Influences of Resonant Wavelengths on Performances of Microcavity Organic Light-Emitting Devices, Appl. Phys. Lett. **90** (7), 2005–2008 (2007). doi:10.1063/1.2472541.

[34] C.C. Wu, C.L. Lin, P.Y. Hsieh, and H.H. Chiang, Methodology for Optimizing Viewing Characteristics of Top-Emitting Organic Light-Emitting Devices, Appl. Phys. Lett. **84** (20), 3966–3968 (2004). doi:10.1063/1.1745107.

[35] G. Liu, X. Zhou, and S. Chen, Very Bright and Efficient Microcavity Top-Emitting Quantum Dot Light-Emitting Diodes with Ag Electrodes, ACS Appl. Mater. Interfaces **8** (26), 16768–16775 (2016). doi:10.1021/acsami.6b03367.

[36] C. Xiang, W. Koo, F. So, H. Sasabe, and J. Kido, A Systematic Study on Efficiency Enhancements in Phosphorescent Green, Red and Blue Microcavity Organic Light Emitting Devices, Light Sci. Appl. **2** (JUNE), 1–7 (2013). doi:10.1038/lsa.2013.30.

[37] W.C.H. Choy, and C.Y. Ho, Improving the Viewing Angle Properties of Microcavity OLEDs by Using Dispersive Gratings, Opt. Express **15** (20), 13288 (2007). doi:10.1364/oe.15.013288.

[38] N. Tessler, S. Burns, H. Becker, and R.H. Friend, Suppressed Angular Color Dispersion in Planar Microcavities, Appl. Phys. Lett. **70** (5), 556–558 (1997). doi:10.1063/1.118207.

[39] W. Lukosz, Light Emission By Multipole Sources in Thin Layers - 1. Radiation Patterns of Electric and Magnetic Dipoles, J. Opt. Soc. Am. **71** (6), 744–754 (1981). doi:10.1364/JOSA.71.000744.

[40] K.A. Neyts, Simulation of Light Emission from Thin-Film Microcavities, J. Opt. Soc. Am. A. **15** (4), 962 (1998). doi:10.1364/josaa.15.000962.

[41] D.S. Leem, S.Y. Kim, J.H. Lee, and J.J. Kim, High Efficiency P-i-n Top-Emitting Organic Light-Emitting Diodes with a Nearly Lambertian Emission Pattern, J. Appl. Phys. **106** (6), (2009) doi:10.1063/1.3225998.

[42] W.H. Choi, H.L. Tam, D. Ma, and F. Zhu, Emission Behavior of Dual-Side Emissive Transparent White Organic Light-Emitting Diodes, Opt. Express **23** (11), A471 (2015). doi:10.1364/oe.23.00a471.